Experimental and Toxicologic Pathology 66 (2014) 1–11

Contents lists available at ScienceDirect

Experimental and Toxicologic Pathology

journal homepage: www.elsevier.de/etp

Immunohistochemical cellular distribution of proteins related to M phase regulation in early proliferative lesions induced by tumor promotion in rat two-stage carcinogenesis models

Atsunori Yafune[a,b], Eriko Taniai[a,b], Reiko Morita[a,b], Hirotoshi Akane[a], Masayuki Kimura[a], Kunitoshi Mitsumori[a], Makoto Shibutani[a,*]

[a] Laboratory of Veterinary Pathology, Tokyo University of Agriculture and Technology, 3-5-8 Saiwai-cho, Fuchu-shi, Tokyo 183-8509, Japan
[b] Pathogenetic Veterinary Science, United Graduate School of Veterinary Sciences, Gifu University, 1-1 Yanagido, Gifu-shi, Gifu 501-1193, Japan

ARTICLE INFO

Article history:
Received 1 March 2013
Accepted 1 July 2013

Keywords:
Carcinogen
M phase
p21^{Cip1}
Two-stage carcinogenesis model
Rat

ABSTRACT

We have previously reported that 28-day treatment with hepatocarcinogens increases liver cells expressing p21^{Cip1}, a G_1/S checkpoint protein, and M phase proteins, i.e., nuclear Cdc2, Aurora B, phosphorylated-Histone H3 (p-Histone H3) and heterochromatin protein 1α (HP1α), in rats. To examine the roles of these markers in the early stages of carcinogenesis, we investigated their cellular distribution in several carcinogenic target organs using rat two-stage carcinogenesis models. Promoting agents targeting the liver (piperonyl butoxide and methapyrilene hydrochloride), thyroid (sulfadimethoxine), urinary bladder (phenylethyl isothiocyanate), and forestomach and glandular stomach (catechol) were administered to rats after initiation treatment for the liver with *N*-diethylnitrosamine, thyroid with *N*-bis(2-hydroxypropyl)nitrosamine, urinary bladder with *N*-butyl-*N*-(4-hydroxybutyl)nitrosamine, and forestomach and glandular stomach with *N*-methyl-*N'*-nitro-*N*-nitrosoguanidine. Numbers of cells positive for nuclear Cdc2, Aurora B, p-Histone H3 and HP1α increased within preneoplastic lesions as determined by glutathione *S*-transferase placental form in the liver or phosphorylated p44/42 mitogen-activated protein kinase in the thyroid, and hyperplastic lesions having no known preneoplastic markers in the urinary bladder, forestomach and glandular stomach. Immunoreactive cells for p21^{Cip1} were decreased within thyroid preneoplastic lesions; however, they were increased within liver preneoplastic lesions and hyperplastic lesions in other organs. These results suggest that M phase disruption commonly occur during the formation of preneoplastic lesions and hyperplastic lesions. Differences in the expression patterns of p21^{Cip1} between thyroid preneoplastic and proliferative lesions in other organs may reflect differences in cell cycle regulation involving G_1/S checkpoint function between proliferative lesions in each organ.

1. Introduction

Carcinogenicity testing using rodent animals is one of the most important endpoints for evaluating the carcinogenic potential of chemicals. However, regular carcinogenic bioassays requiring 1.5 or 2 years for conducting animal experiments are time-consuming and expensive, and require the use of many experimental animals. A number of alternative methods have been developed to predict carcinogenic potential in short-term assays. There are genetically modified animals using transgenic or gene targeting technologies (Eastin, 1998) or medium-term carcinogenesis bioassays (Tamano, 2010). However, these are expensive and time-consuming or have limited target organs. In contrast, recently developed toxicogenomic approaches for the prediction of carcinogenic potential in target organs appear promising (Jonker et al., 2009; Uehara et al., 2011). Unfortunately, toxicogenomic approaches are also expensive and require integrative methodologies between different laboratories sharing an expression database. Thus, there are no commonly used rapid assays for evaluating the carcinogenic potential of chemicals.

It has been reported that nuclear enlargement is occasionally found from the early stages in target cells after repeated administration of carcinogens, irrespective of their genotoxic potential, in toxicity studies using rodent animals (Allen et al., 2004; Adler et al., 2009). This nuclear enlargement is typically observed in the liver and kidney, and often called as cytomegaly in case of liver cells characterized by the presence of hepatocytes that are enlarged due to increased cytoplasmic volume and as karyomegaly when it

* Corresponding author. Tel.: +81 42 367 5874; fax: +81 42 367 5771.
E-mail address: mshibuta@cc.tuat.ac.jp (M. Shibutani).

0940-2993/$ – see front matter © 2013 Elsevier GmbH. All rights reserved.
http://dx.doi.org/10.1016/j.etp.2013.07.001

occurs in renal tubular cells. Recent studies have shown that ochratoxin A, a renal carcinogen that typically induces karyomegaly, induces aberrant expression of cell cycle-related molecules in proximal tubular areas exhibiting karyomegaly (Adler et al., 2009). These observations suggest that this aberrant expression might eventually cause carcinogenicity in association with the development of chromosomal instability. Therefore, we hypothesize that an early event that disrupts cell cycle regulation initiates the carcinogenic response in the molecular mechanism responsible for cytomegaly/karyomegaly development.

We have previously reported that carcinogens that induce cell proliferation after 28-day treatment in rats concurrently increase the number of carcinogenic target cells, irrespective of target organs, suggestive of disrupting spindle checkpoint at M phase that may eventually lead to chromosomal instability linked to carcinogenesis (Taniai et al., 2012a). Further, we performed immunohistochemical analysis of cell cycle-related proteins after 28 days of repeated administration of hepatocarcinogens that do or do not induce cytomegaly in rat liver cells (Yafune et al., 2013a). In that study, we found that hepatocarcinogens, irrespective of their cytomegaly-inducing potential, increased the number of immunoreactive liver cells for $p21^{Cip1}$, a G_1/S checkpoint protein, and Aurora B, a M phase protein, suggestive of increased cell populations undergoing G_1 arrest or showing chromosomal instability, respectively. We also found that hepatocarcinogens that induce liver cell proliferation might cause M phase arrest of hepatocytes, judging from increased cell population expressing nuclear Cdc2, phosphorylated Histone H3 (p-Histone H3) and heterochromatin protein 1α (HP1α), accompanied by apoptosis. Therefore, we hypothesize that disruption of cell cycle regulation may be the common feature of carcinogenic target cells at the early time point before forming preneoplastic or hyperplastic lesions after treatment with carcinogens that induce cell proliferation. In another study that we have recently performed, we found that M phase proteins may be early prediction markers of carcinogens evoking cell proliferation in many target organs in a scheme of 28-day treatment (Yafune et al., 2013b).

It is now important to know whether $p21^{Cip1}$ and M phase proteins play roles in the formation of proliferative lesions during carcinogenic processes. The present study aimed to clarify the involvement of these proteins in the early carcinogenic processes in the formation of preneoplastic or hyperplastic lesions in different target organs. For this purpose, we employed two-stage carcinogenesis models targeting different organs utilizing organ-specific tumor initiator and following promoter to allow selective proliferation of initiated cells forming proliferative lesions in each organ for short-term. We analyzed the immunohistochemical cellular distribution of these proteins at early stages of tumor promotion in the liver, thyroid, urinary bladder, forestomach, and glandular stomach.

2. Materials and methods

2.1. Chemicals

Methapyrilene hydrochloride (MP; CAS No. 135-23-9), *N*-diethylnitrosamine (DEN; CAS No. 55-18-5, >99.0%), and sulfadimethoxine sodium salt (SDM; CAS No. 122-11-2) were purchased from Sigma–Aldrich Japan K. K. (Tokyo, Japan). *N*-Methyl-*N'*-nitro-*N*-nitrosoguanidine (MNNG; CAS No. 70-25-7, >95.0%), *N*-butyl-*N*-(4-hydroxybutyl)nitrosamine (BBN; CAS No. 3817-11-6, >90.0%), and phenylethyl isothiocyanate (PEITC; CAS No. 2257-09-2, ≥97.0%) were obtained from Tokyo Chemical Industry Co. (Tokyo, Japan). Catechol (CC; CAS No. 120-80-9, >99.0%) was purchased from Wako Pure Chemicals Industries (Osaka, Japan). *N*-Bis(2-hydroxypropyl)nitrosamine (DHPN; CAS No. 53609-64-6) was purchased from Nacalai Tesque (Kyoto, Japan). Piperonyl butoxide (PBO; CAS No. 51-03-6, 90%) was obtained from Nagase & Co. (Osaka, Japan).

2.2. Animal experiments

Animals and experimental design were identical to those previously reported (Taniai et al., 2012b). Animal studies were conducted in compliance with the Guidelines for Proper Conduct of Animal Experiments (Science Council of Japan, June 1, 2006) and according to the protocol approved by the Animal Care and Use Committee of the Tokyo University of Agriculture and Technology. Briefly, five-week-old male F344/NSIc rats were purchased from Japan SLC, Inc. (Hamamatsu, Japan) and acclimatized to a powdered basal diet (CRF-1 diet; Oriental Yeast Co., Tokyo, Japan) and tap water ad libitum. They were housed in stainless steel cages in a barrier-maintained animal room on a 12-h light–dark cycle at 23 ± 3 °C with a relative humidity of 50 ± 20%.

After a 1-week acclimatization period, animals were subjected to two-stage carcinogenesis bioassays as described in Fig. 1. To study the liver as the target organ, a medium-term liver bioassay was employed (Shirai, 1997). All animals were initiated with a single intraperitoneal injection of DEN (200 mg/kg body weight). Two weeks later, animals were divided into three groups and fed the basal diet (DEN-alone) or a diet containing either PBO at 20,000 ppm (DEN + PBO) or MP at 1000 ppm (DEN + MP) for 6 weeks. The animals were subjected to a two-thirds partial hepatectomy at week 3. The doses of PBO and MP have been shown to promote induction of preneoplastic lesions as determined by glutathione *S*-transferase placental form (GST-P) in the liver after a 6-week administration in a two-stage model (Horn et al., 1996; Ichimura et al., 2010). To study the thyroid as the target organ, all animals were initiated with a single subcutaneous injection of DHPN (2800 mg/kg body weight). One week later, animals were given drinking water with (DHPN + SDM) or without (DHPN-alone) SDM at 1500 ppm for 4 weeks. This dose of SDM has been shown to promote induction of follicular cell carcinomas after a 13-week administration in a two-stage model (Kemmochi et al., 2012). To study the urinary bladder as the target organ, all animals were initiated with BBN at 500 ppm in drinking water for 4 weeks. Animals were then given either the basal diet (BBN-alone) or a diet containing PEITC at 1000 ppm (BBN + PEITC) for 8 weeks. This dose of PEITC has been shown to promote induction of transitional cell carcinomas for 32-week administration in a two-stage model (Hirose et al., 1998). To study the forestomach and glandular stomach, all animals were initiated with a single gavage of MNNG (150 mg/kg body weight). One week later, animals were fed either the basal diet (MNNG-alone) or a diet containing CC at 8000 ppm (MNNG + CC) for 12 weeks. This dose of CC has been shown to promote induction of both forestomach and glandular stomach carcinomas after a 51-week administration in a two-stage model (Wada et al., 1998). After cessation of tumor promotion, all animals were sacrificed by exsanguination from the abdominal aorta under deep anesthesia and target organs were removed.

Tissue fixation and following preparation for histopathological assessment were described previously (Taniai et al., 2012b).

2.3. Histopathology and immunohistochemistry

From paraffin-embedded tissues of the liver, thyroid, urinary bladder, and stomach (forestomach and glandular stomach), 3-μm sections were stained with hematoxylin and eosin for histopathological examination and subjected to immunohistochemistry.

Immunohistochemistry was performed using the Vectastain® Elite ABC Kit (Vector Laboratories Inc., Burlingame, CA, USA) with

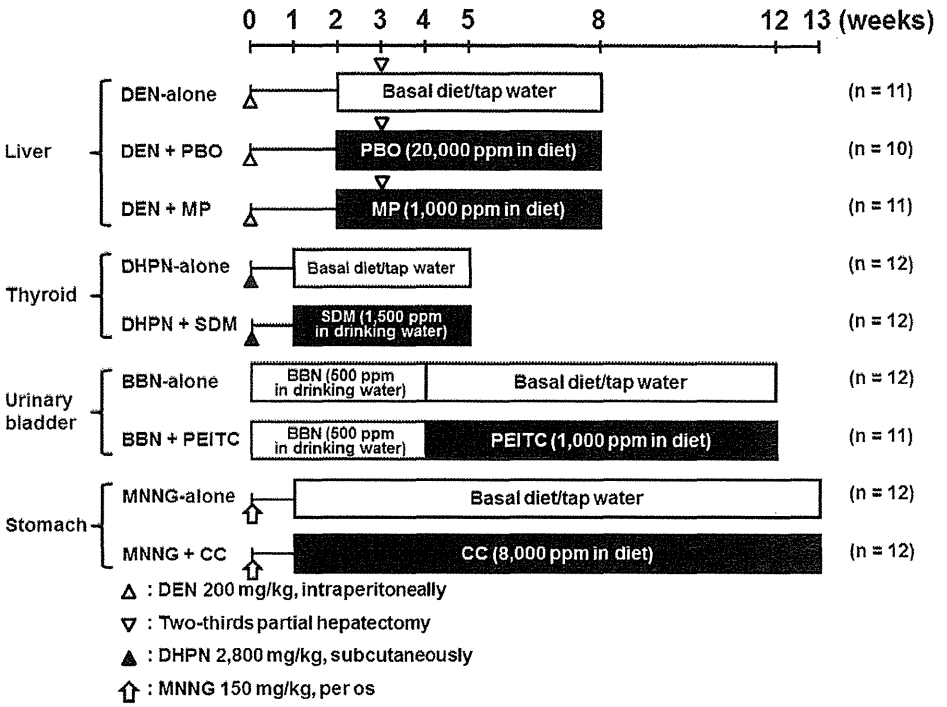

Fig. 1. Experimental design.

3,3′-diaminobenzidine/H_2O_2 as the chromogen. The following primary antibodies were used: $p21^{Cip1}$ mouse monoclonal antibody (1:100; Abcam, Cambridge, UK), Cdc2 mouse monoclonal antibody (1:100; Santa Cruz Biotechnology, Inc., Dallas, TX, USA), Aurora B rabbit polyclonal antibody (1:200; Abcam), p-Histone H3 rabbit polyclonal antibody (Ser 10 phosphorylated, 1:50; Santa Cruz Biotechnology, Inc.), and HP1α rabbit polyclonal antibody (1:200; Cell Signaling Technology, Inc., Danvers, MA, USA).

To detect preneoplastic lesions in the liver and thyroid, the following antibodies were used: glutathione *S*-transferase placental form (GST-P) rabbit polyclonal antibody (1:1000; Medical & Biological Laboratories Co., Ltd, Nagoya, Japan) and phospho-p44/42 mitogen-activated protein kinase (p-Erk1/2; Thr202/Tyr204) rabbit monoclonal antibody (1:400; Cell Signaling Technology, Inc.).

Antigen retrieval was performed in an autoclave for 10 min at 121 °C in 10 mM citrate buffer (pH 6.0) for p-Histone H3 and p-Erk1/2, and in a microwave for 10 min at 90 °C in 10 mM citrate buffer (pH 6.0) for HP1α and $p21^{Cip1}$. Sections were counterstained with hematoxylin for microscopic examination.

2.4. Analysis of immunoreactivity

The number and areas of GST-P^+ liver cell foci larger than 0.2 mm in diameter, and the total areas of the liver sections were measured as described previously (Ichimura et al., 2010). The number and areas of thyroid p-Erk1/2^+ focal follicular cell hyperplasias (FFCHs) consisting of ≥4 cells and the total areas of the thyroid sections were measured. The numbers of cells positive for $p21^{Cip1}$, nuclear Cdc2, Aurora B, p-Histone H3 and HP1α were counted in 10 randomly selected GST-P^+ foci or p-Erk1/2^+ FFCHs at a magnification of 400×. The ratio of positive cells to the total liver or thyroid follicular cells counted was calculated for both the inside and outside regions of the GST-P^+ foci or p-Erk1/2^+ FFCHs. For this purpose, liver cell foci of ≥0.2 mm in diameter and FFCHs consisting of ≥200 cells were selected. The percentage of positive cells was determined in each field. The numbers of immunoreactive cells in the outside regions of the GST-P^+ foci or p-Erk1/2^+ FFCHs were also similarly counted in initiation-alone groups. In the urinary bladder, the numbers of cells positive for $p21^{Cip1}$, nuclear Cdc2, Aurora B, p-Histone H3 and HP1α were counted in 5 randomly selected areas of the urothelium in the BBN-alone group, 5 each of simple hyperplasias, papillary and nodular (PN) hyperplasias and surrounding areas in the BBN + PEITC group at a magnification of 400×, and normalized to the unit length of muscularis mucosae in each field. In the forestomach, the numbers of cells positive for $p21^{Cip1}$, nuclear Cdc2, Aurora B, p-Histone H3 and HP1α were counted in 10 randomly selected areas of the mucosa in the MNNG-alone group, 10 each of hyperplasias and surrounding areas in the MNNG + CC group at a magnification of 400×. The number of positive cells was normalized to the unit length of muscularis mucosae in each field. For the glandular stomach, the numbers of cells positive for $p21^{Cip1}$, nuclear Cdc2, Aurora B, p-Histone H3 and HP1α were counted in 5 randomly selected areas of the pyloric gland epithelia except for proliferative zones in the MNNG-alone group, 5 each of small hyperplastic foci consisting of 4–10 irregular-shaped tubules accompanied with increased cellular density, large hyperplastic foci consisting of glandular epithelial cells often showing goblet cell differentiation, and surrounding tubular epithelia except for proliferative zones in the MNNG + CC group at a magnification of 400×. The ratio of positive cells was estimated and expressed as the percentage of the total number of cells in the hyperplastic foci of each field.

Average of normalized values of immunoreactive cells in different microscopic fields in each animal was estimated for statistical comparison of group data.

2.5. Statistical analysis

For comparison of numerical data between multiple groups, Bartlett's test for equal variance was used to determine whether the variance was homogenous between the groups. If a significant difference in variance was not observed, a one-way analysis of variance (ANOVA) was performed. If significant differences were found, Tukey's test was performed for comparison between the groups. If

a significant difference using Bartlett's test was observed, Steel-Dwass test was performed.

3. Results

3.1. Immunohistochemical cellular distributions in early hepatocarcinogenesis

Nuclear Cdc2$^+$, Aurora B$^+$, p-Histone H3$^+$ and HP1α$^+$ liver cells were sparsely distributed within the liver lobules in the DEN-alone animals. p21^{Cip1+} liver cells were distributed in the perilobular region in the DEN-alone animals. In the PBO and MP-promoted groups, GST-P$^+$ foci in the liver showed higher numbers of cells immunoreactive for p21^{Cip1}, nuclear Cdc2, Aurora B, p-Histone H3 or HP1α than outside the GST-P$^+$ foci of each group (Fig. 2A–E). The numbers of Aurora B$^+$ and p-Histone H3$^+$ cells distributed outside the GST-P$^+$ foci in the PBO- and MP-promoted group were higher than that of the DEN-alone group (Fig. 2C and D). The numbers of p21^{Cip1+} cells distributed outside the GST-P$^+$ foci in the MP-promoted group were higher than that in the DEN-alone group (Fig. 2A). In contrast, there were no obvious differences in the numbers of nuclear Cdc2$^+$ and HP1α$^+$ liver cells distributed outside the GST-P$^+$ foci between the DEN-alone group and PBO- or MP-promoted group (Fig. 2B and E).

3.2. Immunohistochemical cellular distributions in early thyroid carcinogenesis

p21^{Cip1+}, nuclear Cdc2$^+$, Aurora B$^+$, p-Histone H3$^+$ and HP1α$^+$ follicular cells were sparsely distributed in the thyroids of the DHPN-alone animals. In the SDM-promoted group, follicular cells immunoreactive for p21^{Cip1} inside the p-Erk1/2$^+$ FFCHs were significantly lower than outside the p-Erk1/2$^+$ FFCHs (Fig. 3A). In contrast, p-Erk1/2$^+$ FFCHs in the SDM-promoted group showed a higher number of follicular cells immunoreactive for nuclear Cdc2, Aurora B, p-Histone H3 and HP1α than outside the p-Erk1/2$^+$ FFCHs (Fig. 3B–E). The numbers of nuclear Cdc2$^+$, Aurora B$^+$ and HP1α$^+$ cells distributed outside the p-Erk1/2$^+$ FFCHs in the SDM-promoted group were higher than that of the DHPN-alone group (Fig. 3B, C and E). There were no obvious differences in the numbers of p21^{Cip1+} and p-Histone H3$^+$ cells distributed outside the p-Erk1/2$^+$ FFCHs between the SDM-promoted and DHPN-alone groups (Fig. 3A and D).

3.3. Immunohistochemical cellular distributions in early urinary bladder carcinogenesis

Tumor promotion with PEITC resulted in induction of simple hyperplasias and PN hyperplasias of the urothelium in the urinary bladder at week 8. p21^{Cip1+}, nuclear Cdc2$^+$, Aurora B$^+$, p-Histone H3$^+$ and HP1α$^+$ epithelial cells were sparsely distributed in the urothelium of the BBN-alone group. Within the PEITC-promoted group, the numbers of p21^{Cip1+}, nuclear Cdc2$^+$, Aurora B$^+$, p-Histone H3$^+$ and HP1α$^+$ epithelial cells were significantly increased in the simple and PN hyperplasias compared with surrounding epithelial cells (Fig. 4A–E). These immunoreactive cell populations were also significantly increased in the PN hyperplasias compared with the simple hyperplasias. In the PEITC-promoted group, the number of Aurora B$^+$ epithelial cells was significantly increased in the surrounding epithelial cells compared with the urothelium of the BBN-alone group (Fig. 4C).

3.4. Immunohistochemical cellular distributions in early forestomach carcinogenesis

Tumor promotion with CC resulted in induction of hyperkeratosis/parakeratosis and hyperplasias of stratified epithelia in the forestomach at week 12. p21^{Cip1+}, nuclear Cdc2$^+$, Aurora B$^+$, p-Histone H3$^+$ and HP1α$^+$ mucosal epithelial cells were sparsely distributed in the mucosa of the MNNG-alone group. In the CC-promoted group, the numbers of p21^{Cip1+}, nuclear Cdc2$^+$, Aurora B$^+$, p-Histone H3$^+$ and HP1α$^+$ epithelial cells were significantly increased in the surrounding epithelial cells of hyperplastic lesions compared with the mucosa of the MNNG-alone group (Fig. 5A–E). Within the CC-promoted group, the numbers of p21^{Cip1+}, nuclear Cdc2$^+$, Aurora B$^+$, p-Histone H3$^+$ and HP1α$^+$ epithelial cells were significantly increased in the hyperplasias compared with the surrounding epithelial cells.

3.5. Immunohistochemical cellular distributions in early glandular stomach carcinogenesis

Tumor promotion with CC resulted in induction of small and large hyperplastic foci in the glandular stomach at week 12. p21^{Cip1+}, nuclear Cdc2$^+$, Aurora B$^+$, p-Histone H3$^+$ and HP1α$^+$ glandular epithelial cells were sparsely distributed in the pyloric gland epithelia of the MNNG-alone group. In the CC-promoted group, the numbers of p21^{Cip1+} and Aurora B$^+$ glandular epithelial cells were significantly increased in the surrounding glandular epithelial cells of hyperplastic lesions compared with the pyloric gland epithelia of the MNNG-alone group (Fig. 6A and C). Within the CC-promoted group, the numbers of nuclear Cdc2$^+$, p-Histone H3$^+$ and HP1α$^+$ epithelial cells were significantly increased in both the small and large hyperplastic foci compared with the surrounding glandular epithelial cells (Fig. 6B, D and E). These immunoreactive cell populations were significantly decreased in the large hyperplastic foci compared with the small hyperplastic foci. The number of p21^{Cip1+} epithelial cells was significantly increased in the small hyperplastic foci compared with the large hyperplastic foci or the surrounding glandular epithelial cells (Fig. 6A). The number of Aurora B$^+$ epithelial cells was significantly increased in the small hyperplastic foci compared with the surrounding glandular epithelial cells (Fig. 6C).

4. Discussion

In our previous study using the same animals samples of the present study, we have shown immunohistochemical cellular distributions of Ki-67 in the liver, thyroid, urinary bladder, forestomach and glandular stomach (Taniai et al., 2012b). The numbers of Ki-67$^+$ cells were increased in the cells inside the GST-P$^+$ liver cell foci, p-Erk1/2$^+$ thyroid FFCHs, PN hyperplasias of the urinary bladder, mucosal hyperplasias of the forestomach, and small hyperplastic foci of the glandular stomach compared with the surrounding non-preneoplastic or non-hyperplastic cells. In the present study, we found that the numbers of cells positive for nuclear Cdc2, Aurora B, p-Histone H3 and HP1α were significantly increased within the GST-P$^+$ liver cell foci and p-Erk1/2$^+$ FFCHs in the thyroid compared with the surrounding non-preneoplastic cells. In contrast, the numbers of p21^{Cip1+} cells were significantly increased within the GST-P$^+$ liver cell foci; however, in the thyroid, p21^{Cip1+} cells were significantly decreased within the p-Erk1/2$^+$ FFCHs compared with the surrounding non-preneoplastic cells. We also found that the numbers of cells positive for p21^{Cip1}, nuclear Cdc2, Aurora B, p-Histone H3 and HP1α were significantly increased within PN hyperplasias in the urinary bladder, mucosal hyperplasias of the forestomach, and small hyperplastic

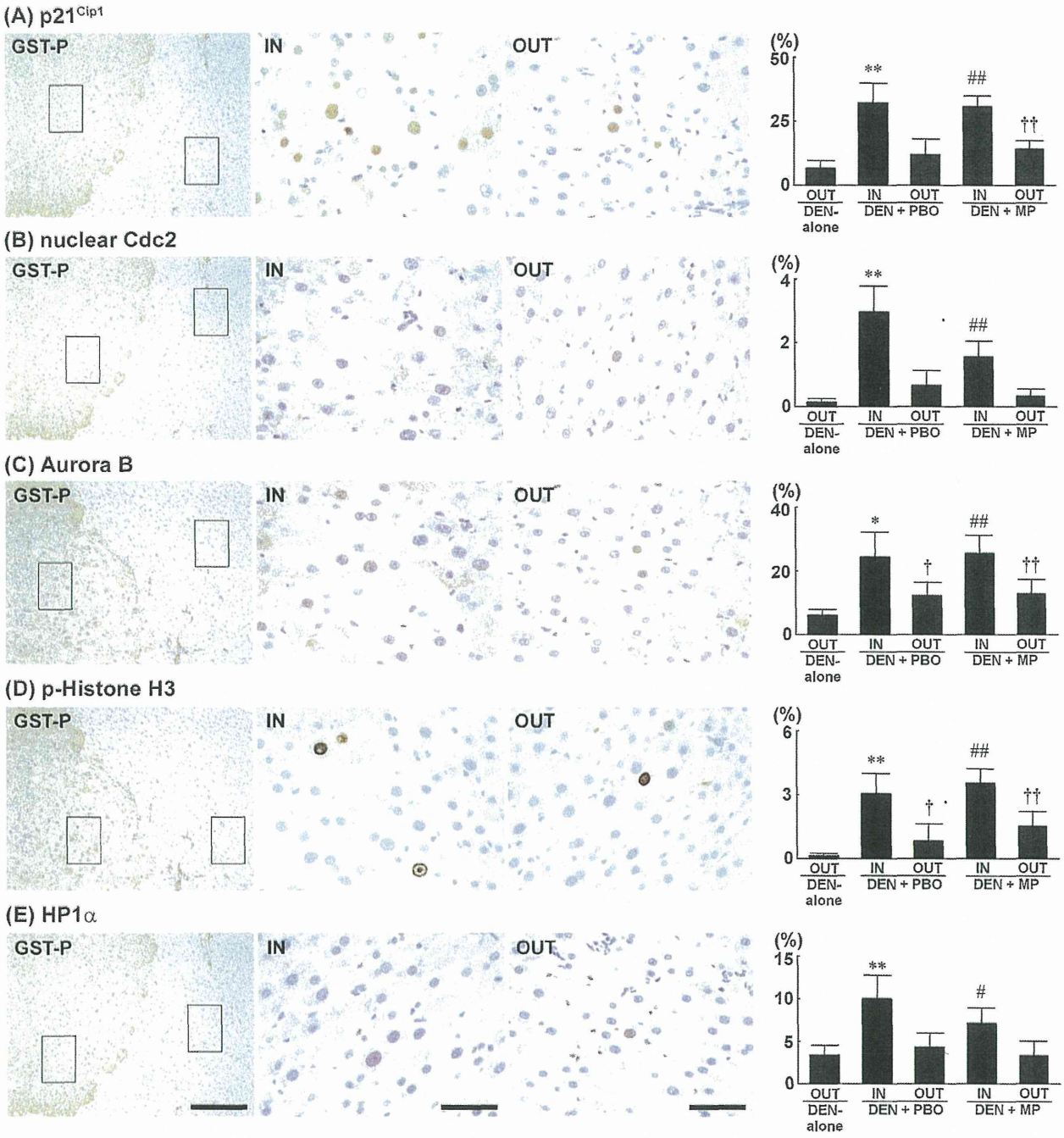

Fig. 2. Distribution of $p21^{Cip1+}$, nuclear $Cdc2^{+}$, Aurora B^{+}, p-Histone $H3^{+}$ and $HP1\alpha^{+}$ cells in early hepatocarcinogenesis. Photomicrographs show the cellular distributions of markers inside and outside the GST-P^{+} foci in the DEN + PBO group. The graphs show positive cell ratios (%) of liver cells inside (IN) and outside (OUT) the GST-P^{+} foci in the DEN + PBO and DEN + MP groups as well as outside the GST-P^{+} foci in the DEN-alone group. Values represent mean + SD. (A) $p21^{Cip1}$, (B) nuclear Cdc2, (C) Aurora B, (D) p-Histone H3, and (E) HP1α. Bar = 200 μm (GST-P), bar = 50 μm (IN, OUT). *, $^{**}P < 0.05$, 0.01 vs. OUT in the DEN + PBO group (Tukey's or Steel-Dwass multiple comparison test). $^{\#,\#\#}P < 0.05$, 0.01 vs. OUT in the DEN + MP group (Tukey's or Steel-Dwass multiple comparison test). $^{\dagger,\dagger\dagger}P < 0.05$, 0.01 vs. OUT in the DEN-alone group (Tukey's or Steel-Dwass multiple comparison test).

foci of the glandular stomach compared with the surrounding non-hyperplastic cells.

In our previous study using the same animals samples of the present study, both the number and areas of GST-P^{+} liver cell foci after 6 weeks of tumor promotion with PBO or MP were significantly increased compared with the DEN-alone group (Taniai et al., 2012b). In the thyroid, FFCHs exhibited positive immunoreactivity for p-Erk1/2 (Taniai et al., 2012b). After 4 weeks of tumor promotion with SDM, both the number and areas of p-$Erk1/2^{+}$ FFCHs were significantly increased compared with the DHPN-alone group (Taniai et al., 2012b). It is generally accepted that preneoplastic lesions induced by tumor promotion have high proliferation activity compared with the surrounding non-neoplastic cells (Ogawa, 2009; Miyamoto et al., 2010). We previously demonstrated that GST-P^{+} liver cell foci and p-$Erk1/2^{+}$ thyroid FFCHs showed high proliferation activity at the early stages of tumor promotion (Taniai et al., 2012b; Shima et al., 2009; Tsuchiya et al., 2012). Both types of lesions are well established

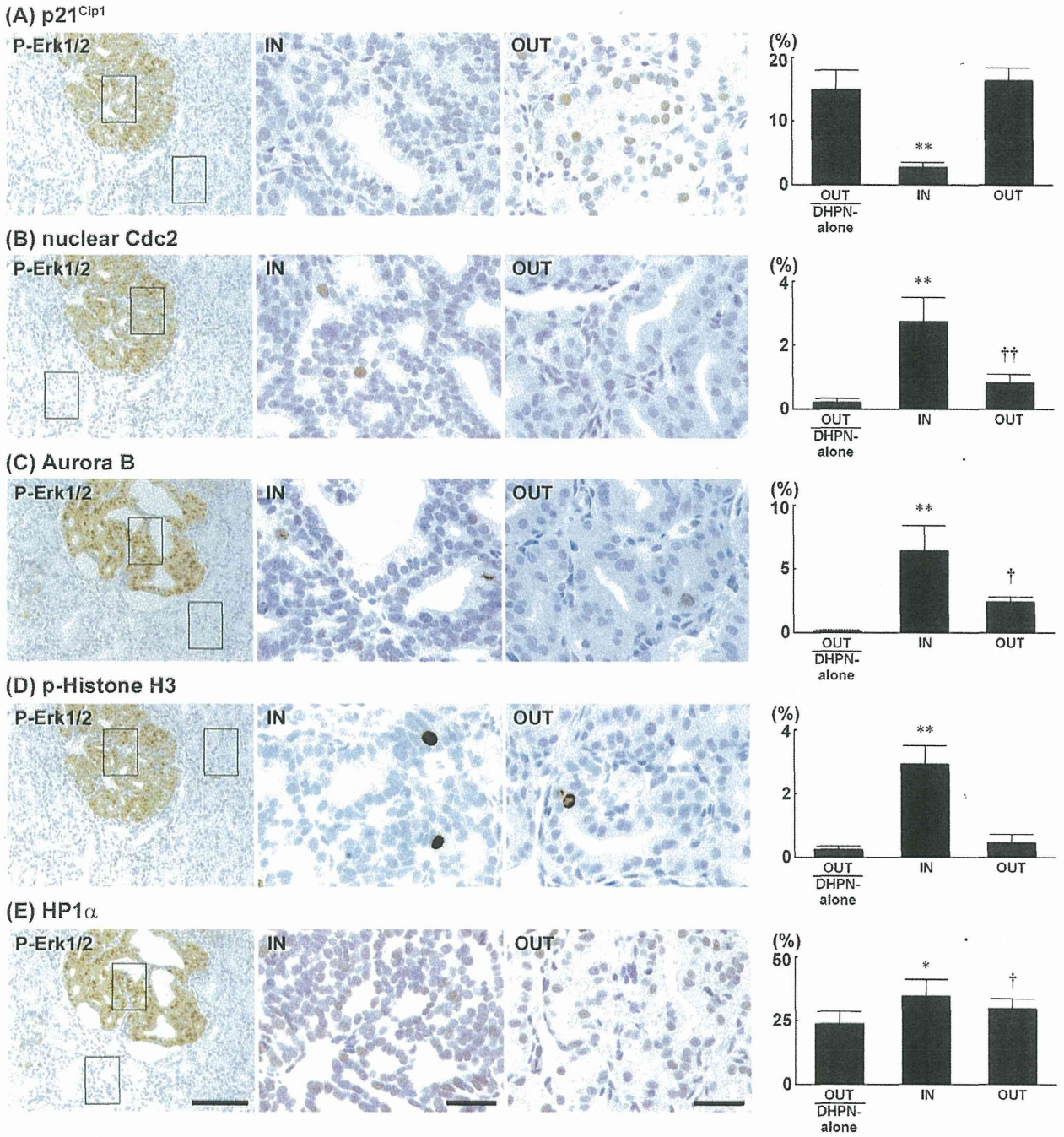

Fig. 3. Distribution of $p21^{Cip1+}$, nuclear $Cdc2^{+}$, Aurora B^{+}, p-Histone $H3^{+}$ and $HP1\alpha^{+}$ cells in early thyroid carcinogenesis. Photomicrographs show the cellular distributions of markers inside or outside the p-Erk1/2^{+} FFCHs in the DHPN + SDM group. The graphs show positive cell ratios (%) of thyroid follicular cells inside (IN) or outside (OUT) the p-Erk1/2^{+} FFCHs in the DHPN + SDM group as well as outside the p-Erk1/2^{+} FFCHs in the DHPN-alone group. Values represent mean + SD. (A) $p21^{Cip1}$, (B) nuclear Cdc2, (C) Aurora B, (D) p-Histone H3, and (E) HP1α. Bar = 100 μm (p-Erk1/2), bar = 30 μm (IN, OUT). *, **$P < 0.05$, 0.01 vs. OUT in the DHPN + SDM group (Tukey's or Steel-Dwass multiple comparison test). †,††$P < 0.05$, 0.01 vs. OUT in the DHPN-alone group (Tukey's or Steel-Dwass multiple comparison test).

as preneoplastic lesions that can develop into neoplastic lesions (Shirai, 1997; Ito et al., 2000; Ago et al., 2010). In contrast, hyperplastic lesions in the urinary bladder, forestomach, and glandular stomach do not have appropriate molecular markers, and they are not established as preneoplastic lesions. In our previous study, we found that ubiquitin D (Ubd) is a cellular marker candidate for the prediction of carcinogenicity in a rat model of 28-day repeated administration (Taniai et al., 2012a). It is known that Ubd leads to chromosomal instability through the reduction of kinetochore localization of spindle checkpoint proteins such as Mad2 during the prometaphase stage (Lim et al., 2006; Herrmann et al., 2007). We previously found no apparent differences in the number of Ubd^{+} cells between inside and outside preneoplastic lesions in the liver and thyroid. However, Ubd^{+} cells were increased within hyperplastic lesions in the urinary bladder, forestomach, and glandular stomach (Taniai et al., 2012b). In contrast, in the present study, cell populations expressing M phase proteins were increased in both the preneoplastic and hyperplastic lesions in all organs examined, suggestive of M phase disruption. Considering the difference in the expression pattern of Ubd between preneoplastic and hyperplastic

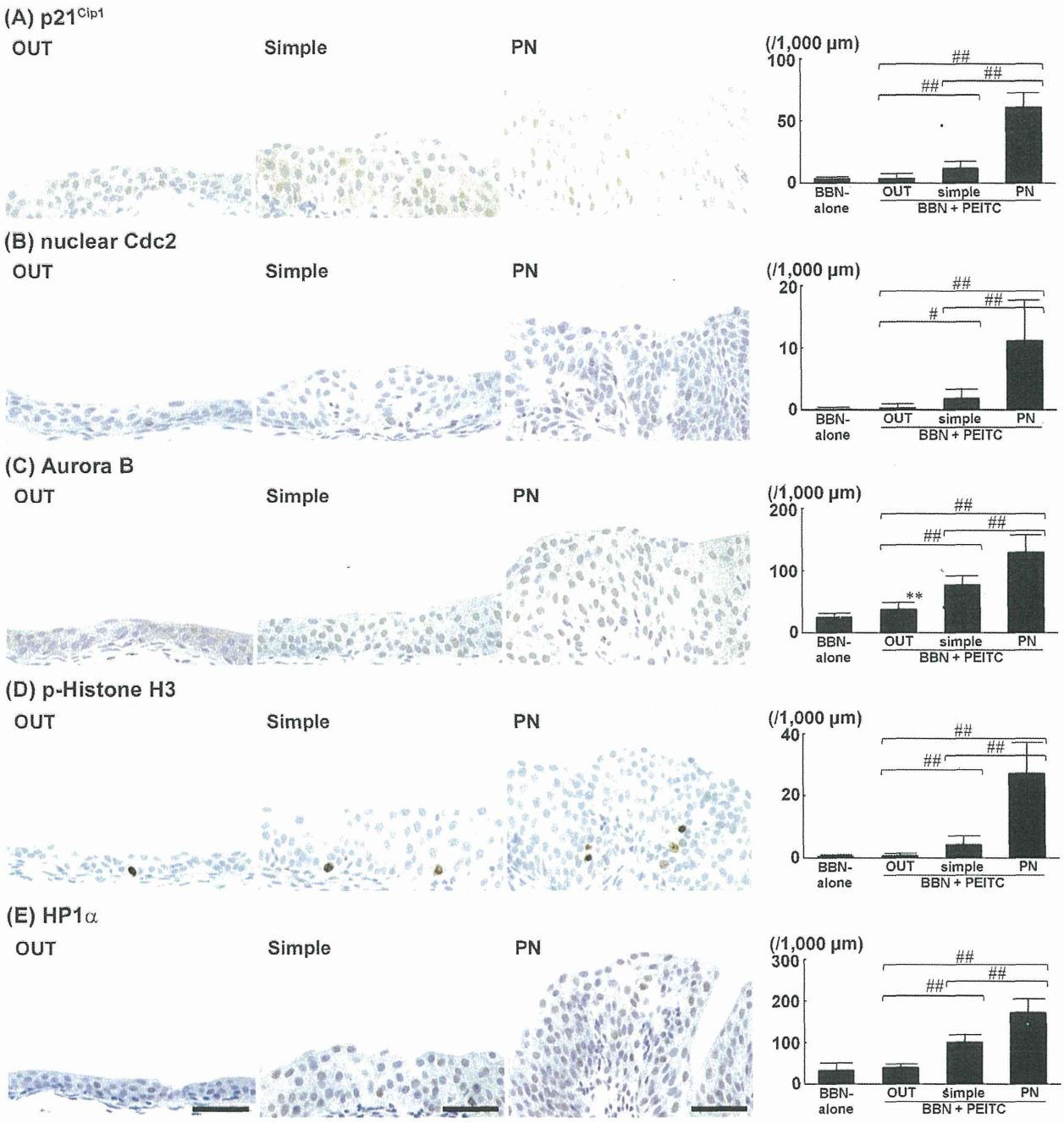

Fig. 4. Distribution of $p21^{Cip1+}$, nuclear $Cdc2^{+}$, Aurora B^{+}, p-Histone $H3^{+}$ and $HP1\alpha^{+}$ cells in early urinary bladder carcinogenesis. Photomicrographs show the cellular distributions of markers in simple hyperplastic foci, PN hyperplastic foci and surrounding epithelial cells in the BBN + PEITC group. The graphs show positive cells per unit muscularis mucosae length (1000 μm) of the urothelium in the BBN-alone group, the surrounding urothelium (OUT), and simple or PN hyperplastic foci in the BBN + PEITC group. Values represent mean + SD. (A) $p21^{Cip1}$, (B) nuclear Cdc2, (C) Aurora B, (D) p-Histone H3, and (E) HP1α. Bar = 50 μm. $^{**}P < 0.01$ vs. the BBN-alone group (Tukey's or Steel-Dwass multiple comparison test). $^{\#,\#\#}P < 0.05$, 0.01 between the groups for comparison (Tukey's or Steel-Dwass multiple comparison test).

lesions, M phase disruption via aberrant activation of Ubd may not be involved in the cellular process of preneoplastic lesions, in contrast to the enhanced activation in hyperplastic lesions compared with surrounding non-hyperplastic cells. Hyperplastic lesions may undergo different carcinogenic steps from those of preneoplastic lesions.

It has been reported that $p21^{Cip1}$ is one of the potent cyclin-dependent kinase inhibitors, which functions as a regulator of cell cycle at G_1 phase (Sherr and Roberts, 1995). In the present study, we found that PBO and MP induced increases in $p21^{Cip1+}$ cells within the GST-P^{+} liver cell foci. Similar to the results in this study, immunohistochemical analysis showed increases in $p21^{Cip1}$ expression in hepatocellular preneoplastic and neoplastic lesions associated with hepatocarcinogenesis in rats (Galand et al., 1988). Expression of $p21^{Cip1}$ is usually regulated by p53 to mediate G_1 arrest (Sherr and Roberts, 1995). However, in the present study, p53 did not respond to promotion with PBO and MP in the liver (data not shown). We previously found that 28-day treatment with hepatocarcinogens induced increases in $p21^{Cip1+}$ cells most likely via Kruppel-like factor 6, a $p21^{Cip1}$ inducer (Abbas and Dutta, 2009), independently of p53 signaling (Yafune et al., 2013a). In contrast, expression of $p21^{Cip1}$ is closely related to

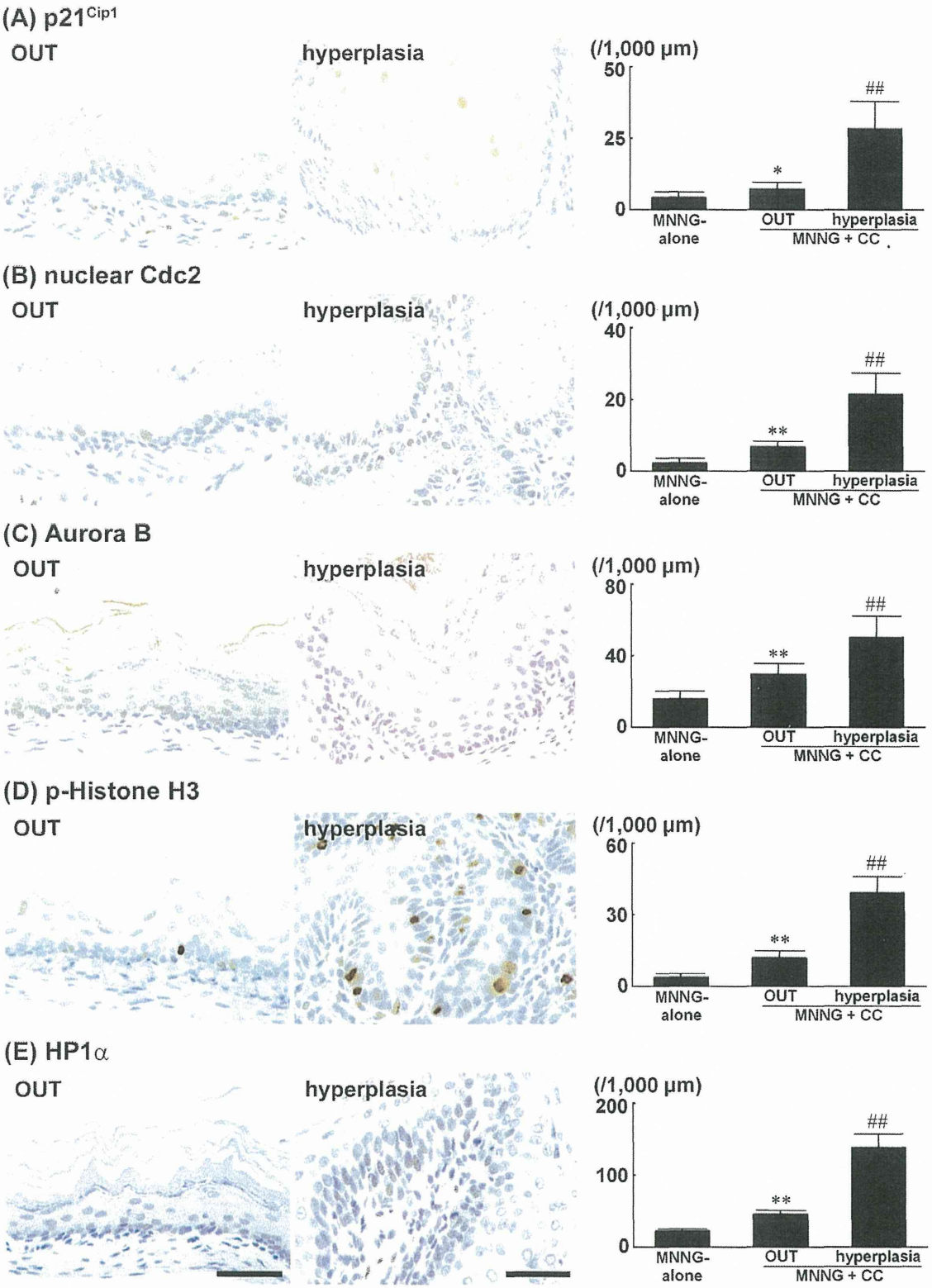

Fig. 5. Distribution of $p21^{Cip1+}$, nuclear $Cdc2^{+}$, Aurora B^{+}, p-Histone $H3^{+}$ and $HP1\alpha^{+}$ cells in early forestomach carcinogenesis. Photomicrographs show the cellular distributions of markers in hyperplasias and surrounding cells in the MNNG + CC group. The graphs show positive cells per unit muscularis mucosae length (1000 μm) of the mucosa in the MNNG-alone group, the surrounding mucosa (OUT) and hyperplasias in the MNNG + CC group. Values represent mean + SD. (A) $p21^{Cip1}$, (B) nuclear Cdc2, (C) Aurora B, (D) p-Histone H3, and (E) HP1α. Bar = 50 μm. *, $^{**}P < 0.05$, 0.01 vs. the MNNG-alone group (Tukey's or Steel-Dwass multiple comparison test). $^{\#\#}P < 0.01$ vs. OUT in the MNNG + CC group (Tukey's or Steel-Dwass multiple comparison test).

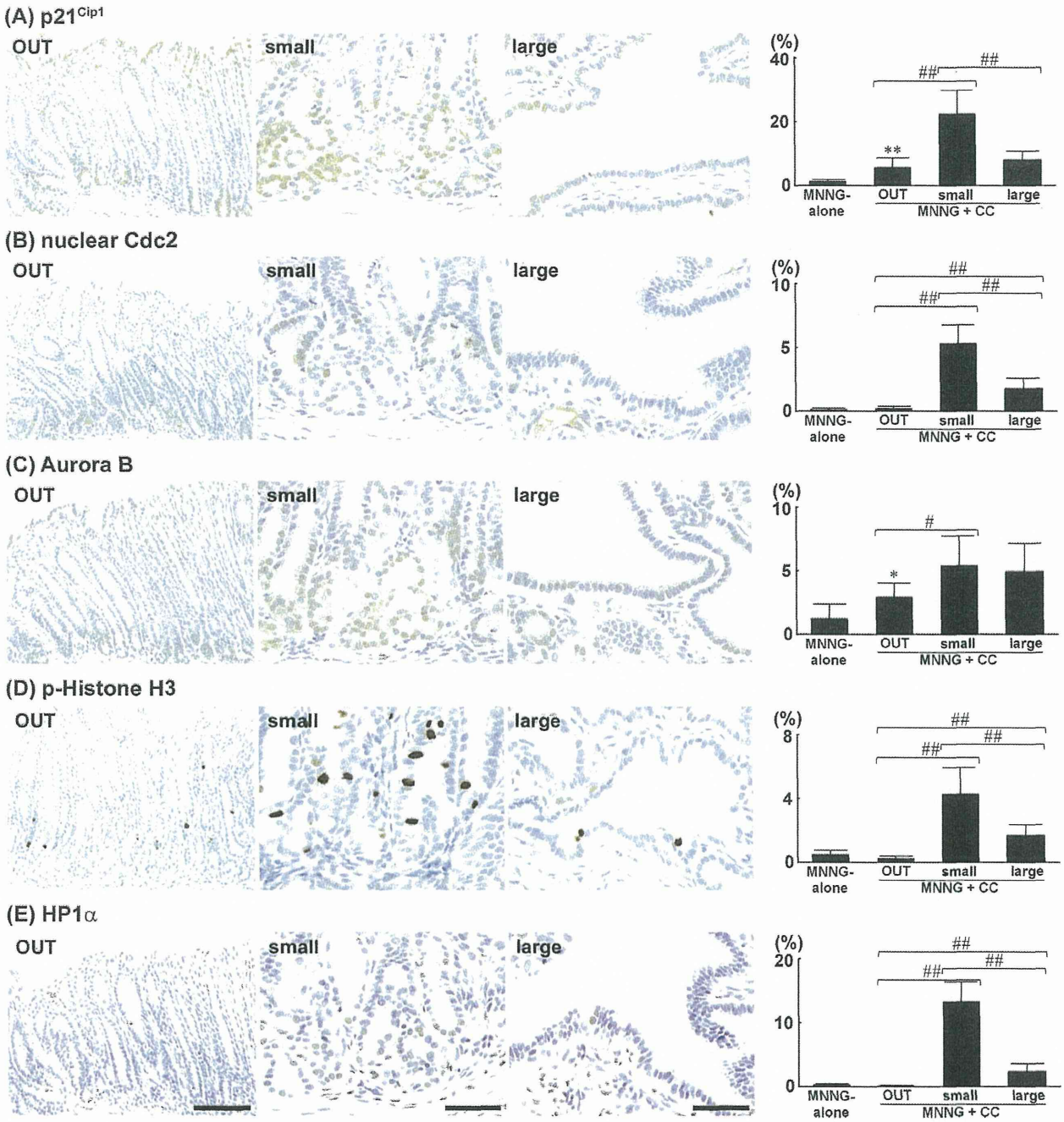

Fig. 6. Distribution of $p21^{Cip1+}$, nuclear $Cdc2^{+}$, Aurora B^{+}, p-Histone $H3^{+}$ and $HP1\alpha^{+}$ cells in early glandular stomach carcinogenesis. Photomicrographs show the cellular distributions of markers in small hyperplastic foci, large hyperplastic foci, and surrounding glandular epithelial cells in the MNNG + CC group. The graphs show positive cell ratios (%) of epithelial cells of the pyloric gland epithelia in the MNNG-alone group, the surrounding glandular epithelial cells (OUT), and in small and large hyperplastic foci in the MNNG + CC group. Values represent mean + SD. (A) $p21^{Cip1}$, (B) nuclear Cdc2, (C) Aurora B, (D) p-Histone H3, and (E) HP1α. Bar = 100 μm (OUT), bar = 50 μm (small, large). *, **$P < 0.05$, 0.01 vs. the MNNG-alone group (Tukey's or Steel-Dwass multiple comparison test). #,##$P < 0.05$, 0.01 vs. between the groups for comparison (Tukey's or Steel-Dwass multiple comparison test).

cellular stress response (Gorospe et al., 1999; Rodriguez and Meuth, 2006). We have previously found that GST-P^{+} foci induced by promotion with hepatocarcinogens including PBO also co-expressed phosphorylated active p38 MAPK (Ichimura et al., 2010). Considering that p38 MAPK is a molecule induced in response to cellular stress (Coulthard et al., 2009), increases in $p21^{Cip1+}$ cells within the GST-P^{+} liver cell foci may reflect activation of G_1/S checkpoint function to undergo G_1 arrest in response to cellular stress via a p53-independent mechanism. Additionally, $p21^{Cip1+}$ cells were also increased within hyperplastic lesions in the urinary bladder, forestomach and glandular stomach, suggestive of increased cell populations arrested at G_1 phase.

In contrast, tumor promotion with SDM induced decreases in $p21^{Cip1+}$ cells within the p-Erk1/2^{+} thyroid FFCHs. It has been reported that $p21^{Cip1}$ directly inhibits the activity of cyclin E/cyclin-dependent kinase (CDK)-2 and cyclin D/CDK4/6 complexes, resulting in suppression of phosphorylation of retinoblastoma protein (Rb), which blocks S-phase entry and causes cell cycle arrest (Xiong et al., 1993; Harper et al., 1993; Niculescu et al., 1998). We previously demonstrated that immunoreactive cells for

phosphorylated Rb in the FFCHs were increased compared with non-neoplastic follicular cells in a two-stage thyroid carcinogenesis model with promotion by 6-propyl-2-thiouracil through the mechanism of hypothyroidism, similarly to SDM in the present study (Ago et al., 2010). These observations suggest that preneoplastic lesions in the thyroid may progress cell cycling and may be considered to acquire a cancerous phenotype in contrast to liver preneoplastic lesions.

In the present study, the number of cells positive for nuclear Cdc2, Aurora B, p-Histone H3 and HP1α were increased within the GST-P$^+$ liver cell foci, p-Erk1/2$^+$ thyroid FFCHs, hyperplastic lesions in the urinary bladder, forestomach and glandular stomach compared with the surrounding non-preneoplastic or non-hyperplastic cells. We have previously found that hepatocarcinogens induce aberrant expression of these M phase proteins (Yafune et al., 2013a). In another study, we have also revealed that carcinogens evoking cell proliferation concurrently induce cell cycle arrest at M phase or showing chromosomal instability reflecting aberration in cell cycle regulation, irrespective of target organs, after 28-day treatment (Yafune et al., 2013b). It has been reported that overexpression of Aurora B causes chromosomal instability in various cancer cells (Qi et al., 2007) and increases in p-Histone H3 as a result of Aurora B overexpression that contributes to chromosome number instability (Ota et al., 2002). Cdc2 and cyclin B form a complex, which initiates the G_2/M transition, and nuclear localization of Cdc2 represents the active isoform entering at the M phase (Kawamoto et al., 1997; Chan et al., 1999). HP1α plays a major role in chromosomal segregation during mitosis (Obuse et al., 2004). Therefore, our previous and present observations suggest that carcinogens induce cell proliferation and cell cycle deregulation reflecting M phase disruption, leading to chromosomal instability in the process of forming hyperplastic or preneoplastic lesions similar to cellular processes resulting after a 28-day administration of carcinogens inducing target cell proliferation.

We have previously found that preneoplastic and hyperplastic lesions increased the number of apoptotic cells (Taniai et al., 2012b). The balance between cell proliferation and apoptosis plays an important role in neoplastic tissue growth (Foster, 2000). In the present study, preneoplastic and hyperplastic lesions showed increases in cell populations of M phase proteins in association with cell proliferation. These results suggest that increased apoptosis in preneoplastic and hyperplastic lesions may occur in relation to M phase disruption during mitosis.

In conclusion, preneoplastic lesions identified by preneoplastic cellular markers in the liver and thyroid and hyperplastic lesions with no known molecular markers in the urinary bladder, forestomach and glandular stomach showed increased numbers of cells positive for nuclear Cdc2, Aurora B, p-Histone H3 and HP1α. These lesions commonly increase cell proliferation activity and cell populations staying at the M phase, and cause chromosomal instability or undergo apoptosis. With regard to p21^{Cip1}, increases in immunoreactive cells within the liver preneoplastic lesions and hyperplastic lesions in the urinary bladder, forestomach and glandular stomach suggest activation of G_1/S checkpoint function causing G_1 arrest. In contrast, decreases in p21^{Cip1+} cells within thyroid preneoplastic lesions suggest activation of cell cycling to acquire a cancerous phenotype.

Conflict of interest statement

All authors disclose that there are no competing financial interests that could inappropriately influence the outcome of this study.

Acknowledgments

The authors thank Mrs. Shigeko Suzuki for her technical assistance in preparing the histological specimens. This work was supported by Health and Labour Sciences Research Grants (Research on Food Safety) from the Ministry of Health, Labour and Welfare of Japan.

References

Abbas T, Dutta A. p21 in cancer: intricate networks and multiple activities. Nature Reviews Cancer 2009;9:400–14.

Ago K, Saegusa Y, Nishimura J, Dewa Y, Kemmochi S, Kawai M, et al. Involvement of glycogen synthase kinase-3β signaling and aberrant nucleocytoplasmic localization of retinoblastoma protein in tumor promotion in a rat two-stage thyroid carcinogenesis model. Experimental and Toxicologic Pathology 2010;62:269–80.

Adler M, Müller K, Rached E, Dekant W, Mally A. Modulation of key regulators of mitosis linked to chromosomal instability is an early event in ochratoxin A carcinogenicity. Carcinogenesis 2009;30:711–9.

Allen DG, Pearse G, Haseman JK, Maronpot RR. Prediction of rodent carcinogenesis: an evaluation of prechronic liver lesions as forecasters of liver tumors in NTP carcinogenicity studies. Toxicologic Pathology 2004;32:393–401.

Chan TA, Hermeking H, Lengauer C, Kinzler KW, Vogelstein B. 14-3-3σ is required to prevent mitotic catastrophe after DNA damage. Nature 1999;401:616–20.

Coulthard LR, White DE, Jones DL, McDermott MF, Burchill SA. p38(MAPK): stress responses from molecular mechanisms to therapeutics. Trends in Molecular Medicine 2009;15:369–79.

Eastin WC. The U.S. National toxicology program evaluation of transgenic mice as predictive models for identifying carcinogens. Environmental Health Perspectives 1998;106:81–4.

Foster JR. Cell death and cell proliferation in the control of normal and neoplastic tissue growth. Toxicologic Pathology 2000;28:441–6.

Galand P, Jacobovitz D, Alexandre K. Immunohistochemical detection of c-Ha-ras oncogene p21 product in pre-neoplastic and neoplastic lesions during hepatocarcinogenesis in rats. International Journal of Cancer 1988;41:155–61.

Gorospe M, Wang X, Holbrook NJ. Functional role of p21 during the cellular response to stress. Gene Expression 1999;7:377–85.

Harper JW, Adami GR, Wei N, Keyomarsi K, Elledge SJ. The p21 Cdk-interacting protein Cip1 is a potent inhibitor of G1 cyclin-dependent kinases. Cell 1993;75:805–16.

Herrmann J, Lerman LO, Lerman A. Ubiquitin and ubiquitin-like proteins in protein regulation. Circulation Research 2007;100:1276–91.

Hirose M, Yamaguchi T, Kimoto N, Ogawa K, Futakuchi M, Sano M, et al. Strong promoting activity of phenylethyl isothiocyanate and benzyl isothiocyanate on urinary bladder carcinogenesis in F344 male rats. International Journal of Cancer 1998;77:773–7.

Horn DM, Jordan WH, Holloway DC, Smith WC, Richardson FC. Dose-dependent induction of GST-P$^+$ staining foci by the rat hepatocarcinogen methapyrilene in the medium-term bioassay. Fundamental and Applied Toxicology 1996;29:194–7.

Ichimura R, Mizukami S, Takahashi M, Taniai E, Kemmochi S, Mitsumori K, et al. Disruption of Smad-dependent signaling for growth of GST-P-positive lesions from the early stage in a rat two-stage hepatocarcinogenesis model. Toxicology and Applied Pharmacology 2010;246:128–40.

Ito N, Imaida K, Asamoto M, Shirai T. Early detection of carcinogenic substances and modifiers in rats. Mutation Research 2000;462:209–17.

Jonker MJ, Bruning O, van Iterson M, Schaap MM, van der Hoeven TV, Vrieling H, et al. Finding transcriptomics biomarkers for *in vivo* identification of (non-)genotoxic carcinogens using wild-type and Xpa/p53 mutant mouse models. Carcinogenesis 2009;30:1805–12.

Kawamoto H, Koizumi H, Uchikoshi T. Expression of the G_2-M checkpoint regulators cyclin B1 and cdc2 in nonmalignant and malignant human breast lesions: immunocytochemical and quantitative image analyses. The American Journal of Pathology 1997;150:15–23.

Kemmochi S, Yamamichi S, Shimamoto K, Onda N, Hasumi K, Suzuki K, et al. Lac color inhibits development of rat thyroid carcinomas through targeting activation of plasma hyaluronan-binding protein. Experimental Biology and Medicine (Maywood, NJ) 2012;237:728–38.

Lim CB, Zhang D, Lee CG. FAT10, a gene up-regulated in various cancers, is cell-cycle regulated. Cell Division 2006;1:20.

Miyamoto S, Yasui Y, Ohigashi H, Tanaka T, Murakami A. Dietary flavonoids suppress azoxymethane-induced colonic preneoplastic lesions in male C57BL/KsJ-db/db mice. Chemico-Biological Interactions 2010;183:276–83.

Niculescu AB III, Chen X, Smeets M, Hengst L, Prives C, Reed SI. Effects of p21(Cip1/Waf1) at both the G1/S and the G2/M cell cycle transitions: pRb is a critical determinant in blocking DNA replication and in preventing endoreduplication. Molecular and Cellular Biology 1998;18:629–43.

Obuse C, Iwasaki O, Kiyomitsu T, Goshima G, Toyoda Y, Yanagida M. A conserved Mis12 centromere complex is linked to heterochromatic HP1 and outer kinetochore protein Zwint-1. Nature Cell Biology 2004;6:1135–41.

Ogawa K. Molecular pathology of early stage chemically induced hepatocarcinogenesis. Pathology International 2009;59:605–22.